Spillover Stabilization of Large Space Structures

Eva A. Czajkowski*
Virgina Polytechnic Institute and State University, Blacksburg, Virginia 24061
Andre Preumont†
Free University of Brussels, 1050 Brussels, Belgium
and
Raphael T. Haftka‡
Virginia Polytechnic Institute and State University, Blacksburg, Virginia 24061

This paper considers the stabilization of the neglected dynamics of the higher modes of vibration in the context of the linear-quadratic-Gaussian controller design. The approach consists of designing observers by directly optimizing a combined cost of spillover margin and standard quadratic performance. Two formulations are proposed. The first optimizes the noise statistics used in the design of the Kalman-Bucy reduced state estimator, and the second optimizes directly the observer gain matrix. A singular value stability robustness test is used to identify the potentially unstable modes. The proposed method can start from an unstable controller and stabilize it through numerical optimization.

Introduction

ACTIVE control of large flexible space structures is typically implemented to control only a few desired modes of vibration. Higher modes, referred to as residual modes, are generally ignored in the design and may be excited by the controller to cause a net destabilizing effect of the system. This is referred to as the spillover phenomenon.[1]

The most straightforward way of alleviating spillover is to increase the passive damping of the residual modes. The same effect can be achieved by supplementing the modal control with direct velocity feedback with collocated sensors and actuators.[2] Alternative techniques have also been suggested.

Balas[3] proposed that a feedthrough component be added to the control that restitutes the original stability margin to a selected number of residual modes. Sesak and Coradetti[4] and Sesak et al.[5] proposed the model error sensitivity suppression (MESS) method, which desensitizes the control system to a given set of neglected modes. Gupta[6] introduced frequency-dependent weighting matrices, which increase the penalty for the high-frequency components of the control, reflecting the fact that input in the frequency range where the model is poor is undesirable. Preumont[7] suggested nonlinear modifications to the control in the vicinity of the equilibrium, which makes the composite system (regulator, observer, and residual modes) benefit from the inherent stability properties of the open-loop system.

Low-order controllers insuring the stability of the full-order system have been investigated by Kwakernaak and Sivan[8] and applied to flutter control by Mukhopadhyay et al.[9] and Newsom and Mukhopadhyay.[10] This method can be used to control a limited set of modes while keeping the others barely stable. Ridgely and Banda,[11] Doyle and Stein,[12] and Kissel and Hegg[13] suggested that spillover stability could be achieved by the loop-transfer recovery (LTR) technique by designing a regulator that satisfies a robustness test and making the controller "recover" the loop-transfer matrix of the regulator, assuming that the noise enters the plant at the input. This technique was applied in Ref. 14 to the design of attitude control and vibration suppression in large space structures. Balas et al.[15] suggested the use of residual-mode filters for the same purpose.

A comprehensive evaluation of the various methods is out of the scope of this paper. The present paper considers the design of controllers with improved spillover stability margins. It is based on the following premises.

1) The structural dynamicist will be able to predict more vibration modes than would be practical to include in the full-order linear-quadratic Gaussian (LQG) control design model, and their knowledge can be used in the design process. (Note, however, that the important task of selection of the reduced model is not addressed in this paper.)

2) The noise statistics involved in the Kalman-Bucy filter (KBF) design can, at least to some extent, be used as free parameters to achieve appropriate observer properties. This point of view is also taken in MESS and LTR.

Based on these premises, an optimization problem can be formulated in which the elements of the plant noise intensity matrix are used as design variables to minimize a composite performance index with contributions from both performance and spillover. An alternative formulation, in which the observer gains are used as design variables, is also presented.

Spillover and Residual Modes Selection

Spillover Phenomenon

In what follows, the modal amplitudes and reduced modal velocities are used as state variables, and the subscripts c and r refer to the controlled and residual modes, respectively. With classical control notation, the equations of motion of the complete structure are:

$$\dot{x}_c = A_c x_c + B_c u + w_1 \tag{1}$$

$$\dot{x}_r = A_r x_r + B_r u \tag{2}$$

$$y = C_c x_c + C_r x_r + w_2 \tag{3}$$

where w_1 and w_2 are the plant and measurement noise, with intensity matrices W_1 and W_2, respectively. It is assumed that there is *perfect knowledge* of the dynamics of the n_c controlled modes. The residual modes are not included in the design of

Presented as Paper 88-2484 at the AIAA SDM Issues of the International Space Station, Williamsburg, VA, April 18-20, 1988; received Nov. 3, 1988; revision received Aug. 3, 1989.

*Graduate Research Assistant, Department of Aerospace and Ocean Engineering. Member AIAA.
†Professor, Department of Applied Mechanics. Member AIAA.
‡Christopher Kraft Professor of Aerospace and Ocean Engineering. Member AIAA.

the controller. [This is why no noise term need be considered in Eq. (2).]

The controller consists of two parts. The first is an observer used to estimate the state of the system that, in general, is not fully known. The estimated state $\hat{x}_c$ is obtained by integrating

$$\dot{\hat{x}} = A_c\hat{x}_c + B_c u + K_c(y - C_c\hat{x}_c) \qquad [\hat{x}_c(0) = 0] \tag{4}$$

where K_c is the observer gain matrix.

The second part of the controller is a regulator with control law $u = -G_c\hat{x}_c$.

In the LQG controller design, the regulator and observer gain matrices G_c and K_c are determined to minimize the quadratic performance index

$$J = E\left[x_c^T Q x_c + u^T R u\right] \tag{5}$$

where $Q \geq 0$ is related to the required performance of the output and $R > 0$ is related to the control cost. It is well known[8] that G_c and K_c can be determined independently by solving two Riccati equations, one for the regulator (LQR) and one for the observer (KBF).

The effect of the residual modes can be analyzed by considering the composite system where the state vector also includes the estimation error $e_c = \hat{x}_c - x_c$ and the residual modes, i.e., $(x_c^T e_c^T x_r^T)^T$. The corresponding governing equation for this system becomes

$$\begin{bmatrix} \dot{x}_c \\ \dot{e}_c \\ \dot{x}_r \end{bmatrix} = \begin{bmatrix} A_c - B_c G_c & -B_c G_c & 0 \\ 0 & A_c - K_c C_c & K_c C_r \\ -B_r G_c & -B_r G_c & A_r \end{bmatrix} \begin{bmatrix} x_c \\ e_c \\ x_r \end{bmatrix} \tag{6}$$

This equation is the starting point for analyzing spillover (Fig. 1). The key terms in spillover are $-B_r G_c$ and $K_c C_r$. They arise from the sensor output being contaminated by the residual modes via the term $C_r x_r$ (observation spillover) and the feedback control exciting the residual modes via the term $B_r u$ (control spillover).

From Eq. (6), it can be seen that if either $C_r = 0$ or $B_r = 0$, the eigenvalues of the system are decoupled and are those of the regulator $(A_c - B_c G_c)$, the observer $(A_c - K_c C_c)$, and the residual modes (A_r). They are typically located in the complex plane as indicated in Fig. 2. The poles of the regulator (controlled modes) have a substantial stability margin, and the observer poles are located on their left side. On the contrary, the poles corresponding to the residual modes are stable but close to the imaginary axis; the small stability margin is provided by the natural damping.

When both $C_r \neq 0$ and $B_r \neq 0$, i.e., both observation and control spillover are present, the eigenvalues of the system shift away from $A_c - B_c G_c$, $A_c - K_c C_c$, and A_r. The magnitude of this shift depends on $-B_r G_c$ and $K_c C_r$. Since the poles of A_r have a small stability margin due to the low structural damping, even a slight shift from this position can bring these poles into the right-half side of the complex plane and, thus, make the system unstable. This phenomenon is called spillover instability.

Not all of the residual modes are potentially critical from the point of view of spillover, but only those that are observable, controllable, and close to the bandwidth of the controller. How these modes can be identified is discussed in the next section.

Marginal vs Robust Residual Modes

Stability robustness tests[11, 12] may provide some insight as to which residual modes are potentially critical for spillover. These tests try to quantify the effect of modeling errors on stability and are especially useful for the analysis of the effect of the truncated dynamics.

Doyle and Stein[12] developed robustness tests where the modeling errors were represented by multiplicative unstructured uncertainties. A multiplicative unstructured uncertainty at the plant output $L(j\omega)$, (Fig. 3), is represented by

$$\tilde{G}(j\omega) = \left|I + L(j\omega)\right| G(j\omega) \tag{7}$$

where $\tilde{G}$ and G are, respectively, the actual and model transfer matrices of the plant.

If $\ell_m(\omega)$ is an upper bound on the maximum singular value of the multiplicative uncertainty at the plant output,

$$\bar{\sigma}\left|L(j\omega)\right| < \ell_m(\omega) \tag{8}$$

the stability robustness of the control system is guaranteed if the maximum singular value of the loop-transfer matrix satisfies the inequality

$$\bar{\sigma}\left\{G(j\omega)K(j\omega)\left[I + G(j\omega)K(j\omega)\right]^{-1}\right\} < 1/\ell_m(\omega) \tag{9}$$

where $K(j\omega)$ is the compensator transfer matrix:

$$K(j\omega) = G_c(j\omega I - A_c + B_c G_c + K_c C_c)^{-1} K_c \tag{10}$$

In the frequency range where $\ell_m(\omega) \gg 1$, which is typically in the frequency range where the model has been truncated, inequality (9) can be reduced to

$$\bar{\sigma}\left|G(j\omega)K(j\omega)\right| < 1/\ell_m(\omega) \tag{11}$$

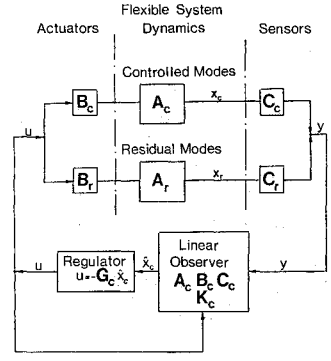

Fig. 1 Spillover mechanism.

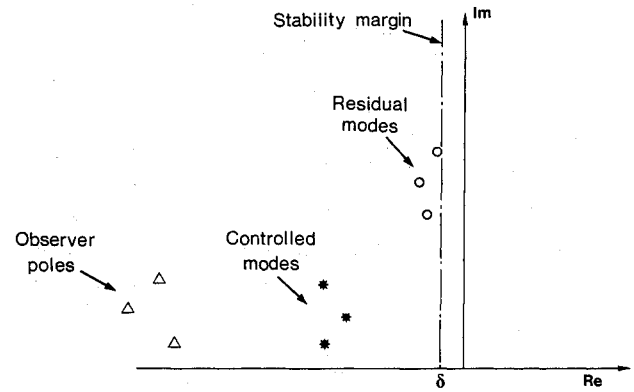

Fig. 2 Location of the closed-loop poles in the complex plane (only upper half is shown).

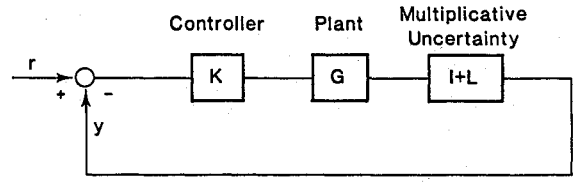

Fig. 3 Unity feedback configuration with multiplicative uncertainty at the plant output.

Similar tests exist if the uncertainty is assumed at the input.[11,12]

Since an accurate structural model is assumed to be available, an obvious way to evaluate the multiplicative uncertainty due to the truncated dynamics is (assuming a square G matrix)

$$L(j\omega) = \tilde{G}(j\omega)G^{-1}(j\omega) - I \tag{12}$$

where

$$G(j\omega) = \left[C_c(j\omega I - A_c)^{-1}B_c\right]_{\text{controller model}} \tag{13}$$

$$\tilde{G}(j\omega) = \left[C(j\omega I - A)^{-1}B\right]_{\text{best available model}} \tag{14}$$

However, due to the large size of the structural model, there are numerical problems associated with the calculation of Eq. (14). In fact, for vibrating structures with classical damping, it is easier to evaluate the *additive* uncertainty, which can be readily written as the sum of its modal contributions in the form

$$G = \sum_{i=1}^{m} h_i(\omega)\phi_i(s)\phi_i^T(a) \tag{15}$$

$$\Delta G = \sum_{i=m+1}^{\infty} h_i(\omega)\phi_i(s)\phi_i^T(a) \tag{16}$$

where the first sum extends over all the modes included in the control model and the second one over all the available modes excluded from the model. In these relationships, $h_i(\omega) = \{\mu_i[(\omega_i^2 - \omega^2) + 2j\xi_i\omega_i\omega]\}^{-1}$ is the transfer function for the mode i, and $\phi_i(s)$ and $\phi_i(a)$ are the vectors of modal amplitudes at the sensor and actuator locations, respectively. A slightly different form applies when there are rate sensors.

Using singular value inequalities, the following upper bound $\ell_m(\omega)$ is readily obtained:

$$\bar{\sigma}[L(j\omega)] \le \frac{\bar{\sigma}[\Delta G(j\omega)]}{\underline{\sigma}[G(j\omega)]} \equiv \ell_m(\omega) \tag{17}$$

where $\underline{\sigma}$ stands for the minimum singular value.

The robustness criteria are sufficient but not necessary conditions for stability since the tests do not take into account the structure of the uncertainty, e.g., phase angles. They are based on a worst case, which is not necessarily allowed by the structure of the system, and tend to be, in our experience, quite pessimistic. As a result, if the robustness tests are violated, it does not mean that the system is going to be unstable but rather that it may become unstable. A typical robustness plot is shown in Fig. 4. It refers to the beam example, which will be discussed later in the paper. The uncertainty curve, and particularly the negative peaks, depend on the damping ratio of the neglected modes. Because of the relatively slow decay rate of $\bar{\sigma}[G(j\omega)K(j\omega)]$ outside the bandwidth of the controller and the low damping ratio, the robustness test cannot, in general, be satisfied by the uncontrolled modes directly outside the bandwidth of the controller unless there is a gap in the natural frequencies of the structure. The marginal modes that are in that transition region (residuals) are candidates for destabilization and must be considered in the spillover analysis. Only the controlled and the marginal residual modes will have to be considered in the remainder of this study; the latter will be called residual modes. The uncontrolled modes that satisfy the robustness test with an appropriate margin will be called robust modes and will be ignored in what follows.

Observer Design for Spillover Stabilization

Effect of Noise Statistics

The noise environment is defined by the noise intensity matrices W_1 and W_2. For a given (W_1, W_2), the optimum observer for the reduced model is the KBF. Often we do not know W_1 and W_2 accurately and, even if we do, it may be advantageous to use different noise matrices in the design of the observer. Examples of that are given by MESS[5] and LTR.[11] In the former, the measurement noise intensity matrix used in the KBF design is taken of the special form

$$V_2 = C_r C_r^T \tag{18}$$

to generate an observer that is blind, to some extent, to the residual modes. In the latter, the plant noise is assumed to enter at the input:

$$V_1 = g^2 B_c B_c^T \tag{19}$$

It has been shown that for minimum phase systems, when $g^2 \to \infty$, the loop-transfer matrix approaches that of the regulator, with the associated guaranteed stability margins. (This, however, brings no improvement—on the contrary—to the slow decay rate of $\bar{\sigma}[GK]$ at high frequency, which is the basic reason for the robustness failure in the present study; see Fig. 4.)

Let V_1 and V_2 be, respectively, the plant noise and measurement noise intensity matrices used in the design of the KBF. When V_1 and V_2 are different from W_1 and W_2, the resulting KBF is no longer optimum with respect to the given noise environment. However, typically the performance index [Eq. (5)] is not overly sensitive to the choice of (V_1, V_2) for a wide range of values, i.e., the optimum is rather flat. In addition, it has been demonstrated[16] that the choice of (V_1, V_2) can have a strong influence on the stability margin of the residual modes. Therefore, it is reasonable to select V_1 and V_2 so as to suppress spillover instability as long as the performance of the KBF is not overly compromised.

The performance index of the stochastic linear quadratic regulator (LQR) in Eq. (5) can be evaluated from the solution of an $n \times n$ Riccati equation. When the LQR is implemented on the reconstructed state from an observer, there is an additional penalty resulting from the imperfect knowledge of the state. The new value of the performance index J can be evaluated by solving a $2n \times 2n$ Lyapunov equation.

In the following, the observer performance is measured by the ratio

$$F_{\text{performance}} = \frac{J - J_{\text{LQR}}}{J_{\text{LQR}}} \ge 0 \tag{20}$$

where J and J_{LQR} are evaluated with the actual noise statistics (W_1, W_2), and not those taken in the design of the KBF (V_1, V_2), so that $F_{\text{performance}}$ represents the performance deterioration for the actual noise statistics. It is minimum for $(V_1, V_2) = (W_1, W_2)$.

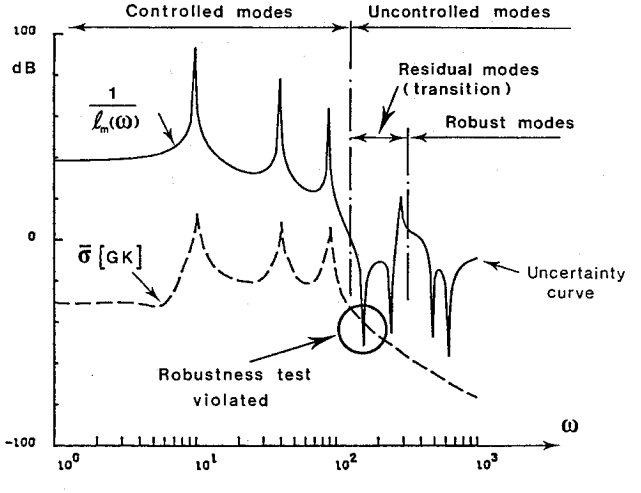

Fig. 4 Robustness plot for the beam example; the uncertainty curve corresponds to modes 4-8, $\xi = 0.001$.

Optimization of Noise Intensity Matrices

The observer is obtained as the KBF whose plant noise intensity matrix V_1 is the solution of the following optimization problem.

Find V_1 and a stability margin δ to minimize

$$F = (\delta - t)_+^2 + \mu F_{\text{performance}} \tag{21}$$

subject to the constraints on the residual modes eigenvalues λ_i

$$\text{Re}(\lambda_i) < \delta \tag{22}$$

The parameter μ is used to weight the objectives of spillover stability and performance, and t is the minimum desired stability margin. The parameter δ is the stability margin for the residual modes chosen by the optimization procedure, and its final value is the actual stability margin (Fig. 2). The notation $(\ )_+$ stands for $(\bar{a})_+ = \max(\bar{a}, 0)$. The spillover part does not contribute to the objective function if the real parts of all the poles are smaller than t. In that case, the design is based on performance only.

In the preceding procedure, the measurement noise intensity matrix V_2 can be taken either according to MESS,[4,5] so as to minimize the observation spillover, or set equal to W_2, the actual noise.

Note that if t is selected in such a way that $t > \delta$, the spillover part $(\delta - t)_+$ vanishes and we optimize performance only. For that case, if $V_2 = W_2$, the optimum solution corresponds to the optimum observer, which minimizes J in Eq. (20). This is the KBF corresponding to (W_1, W_2); therefore, our V_1 will converge to W_1. The same conclusion holds for extremely large μ causing the performance term to be dominant in Eq. (21), and the spillover term to be negligible.

To reduce the number of design variables, V_1 was assumed to be either diagonal, $V_1 = \text{diag}(v_i^2)$, or an outer product matrix of rank one, $V_1 = aa^T$. This reduces the number of design variables in the optimization to $n + 1$. For the examples that we investigated, it was observed in Ref. 16 that these special forms of V_1 produced virtually the same improvements in spillover alleviation as the full V_1 (the optimum full V_1 turned out to be very close to a matrix of rank one). Special forms assuming that the plant noise enters at the input have also been tried, but have not been found very effective in this study.

Direct Design of Observer Gain Matrix

In the foregoing formulation, the observer gain matrix is obtained as a KBF with noise intensity matrices V_1 and V_2. It requires the solution of a nonlinear matrix Riccati equation within the optimization process, which may become difficult if the dimension of the system becomes large. An alternative formulation for the observer design, which does not require multiple solutions of the Riccati equation, is to take the elements of the observer gain matrix K_c as design variables instead of the elements of V_1.

The KBF corresponding to the actual noise statistics (W_1, W_2), is taken as a starting point. If all the residual modes (those identified as failing the robustness test) satisfy the condition

$$\text{Re}(\lambda_i) < t \tag{23}$$

an optimum solution has been found. If condition (23) is not satisfied, the observer gain matrix K_c is obtained as the solution of the following optimization problem.

Find K_c and a stability margin δ to minimize

$$F = (\delta - t)_+^2 + \mu F_{\text{performance}} \tag{24}$$

subject to the constraints

$$\text{Re}(\lambda_i) < \delta \tag{25}$$

The only difference with respect to the preceding problem is a change of design variables. The resulting observer will no longer be a KBF [unless condition (23) is satisfied] and will not enjoy its properties.

The benefit of the foregoing formulation is that the solution of the Riccati equation is not required anymore within the optimization process. The evaluation of the objective function requires only the solution of the linear matrix Lyapunov equation. The number of design variables is now $nm + 1$, where m is the number of outputs of the system.

Again, a stable solution cannot be guaranteed, but the optimal value of δ, if positive, gives approximately the minimum amount of passive damping that is necessary to achieve stability. (This is approximate because passive damping would introduce additional coupling of controlled and residual modes not included in the analysis.) If it is judged too large, the value of μ may be reduced in the objective function, to put less emphasis on performance and more on spillover.

The NEWSUMT-A program[17] was used for optimization where the derivatives of the constraints and the objective function were calculated by finite differences. The L-A-S program[18] was used for control calculations.

Examples

Beam

The beam example used by Balas[1] to demonstrate spillover is used to demonstrate the proposed method. The simply supported beam is controlled by one actuator located at the 1/6 position and a displacement sensor located at the 5/6 position. The first three modes are controlled by the same LQR as in Ref. 1 ($R = 0.2$, Q selected so that x^TQx represents system energy), and the foregoing procedure is used to design a KBF that stabilizes the neglected dynamics. The robustness plot requires the assumption of some structural damping. We assumed $\xi = 0.001$ for the robustness plots. However no damping was assumed for the spillover calculations. Figure 4 shows the robustness plot for a typical design, with the uncertainty curve drawn using the first eight modes. It can be seen that the fourth mode fails the robustness test and must be considered explicitly. The robustness of modes 5 and above can be concluded from this curve and, thus, are not considered further, except for a check with the final design. Note also that the sixth mode is neither controllable nor observable and has no negative peak associated with it in the $1/\ell_m$ curve.

The actual noise statistics were assumed to be $W_1 = I$ and $W_2 = 0.02$. For the optimization, t was taken to equal -0.100 s^{-1}, and V_2 was taken as equal to W_2, the actual measurement noise. A tracing method was used for each of the designs, i.e., the optimum V_1 (or K_c) for one value of μ was used as the initial solution for the next value of μ. Without tracing, the optimum was found to depend appreciably on the initial conditions (local optimum).

The results for the observer design based on optimizing the matrices V_1 and K_c are given in Fig. 5 as a function of the weighting parameter μ. As expected, as μ decreases in value, the performance index J increases in magnitude. This indicates a deterioration in performance. At the same time, the system stability margin increases since the optimizer places more emphasis on a stable system at the cost of performance.

The design $V_1 = aa^T$ is more effective than $V_1 = \text{diag}(v_i^2)$ even though both have six design variables. The case $V_1 = aa^T$ fully populates the V_1 matrix, and for a given δ, produces designs that give J that are appreciably lower than those of the $V_1 = \text{diag}(v_i^2)$ design. The $V_1 = aa^T$ design also gives much slower observers than the $V_1 = \text{diag}(v_i^2)$ design. These differences are most obvious when μ is small.

The K_c designs are comparable in performance (δ vs J) to those of the $V_1 = aa^T$ designs. The resulting observer speeds are also comparable. The δ vs J curve obtained by optimizing K_c should be to the left of the $V_1 = aa^T$ curve because any design obtained by optimizing V_1 can also be obtained by optimizing

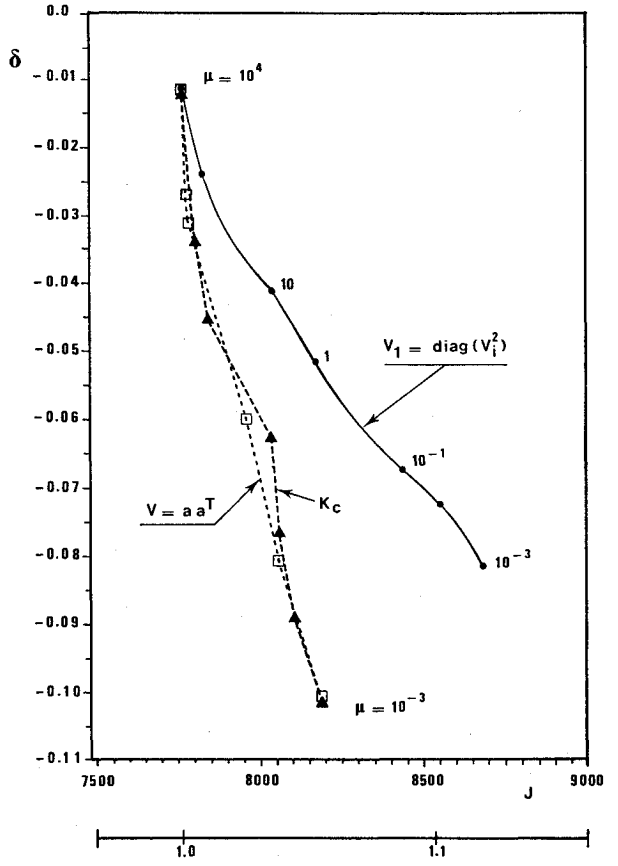

Fig. 5 Stability margin δ vs performance index J for various designs (beam example).

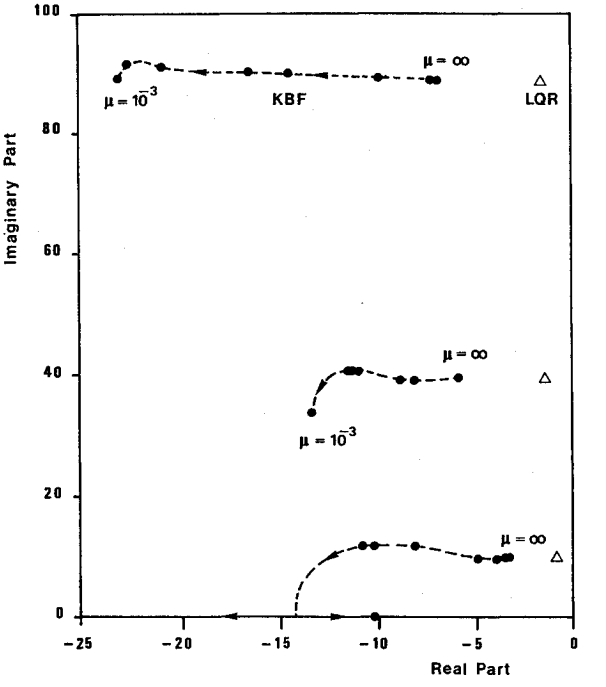

Fig. 6 Evolution of the closed-loop poles as functions of μ; $\mu = \infty$ corresponds to the stochastic optimum (only upper half is shown).

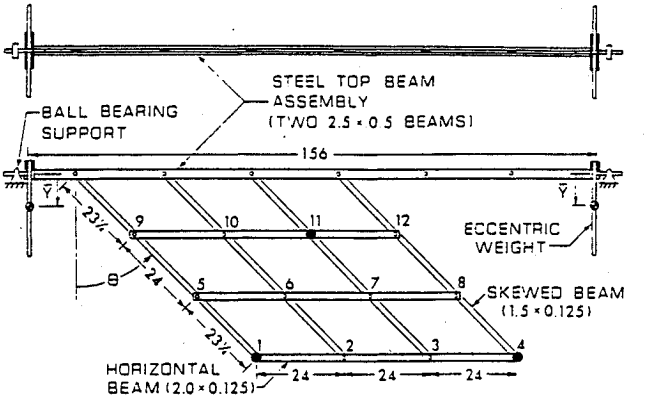

Fig. 7 Grid structure (all dimensions in inches); collocated actuators and displacement sensors are assumed at nodes 1, 4, and 11.

K_c. This holds for only part of the curve. The differences between the curves amount to less than 1% in the objective function, and NEWSUMT-A is not that sensitive. The $V_1 = aa^T$ case picks up most of the stability margin with low performance deterioration. The only advantage of the K_c formulation, in this case, is that it does not require the solution of the nonlinear matrix Riccati equation. However, this is not important for this low-order problem.

Also, although not apparent from Fig. 5, the KBF design noise matrices correspond to the actual noise matrices for extremely large values of μ, i.e., a heavy penalty is placed on performance in the optimization process. Figure 6 shows the evolution of the closed-loop poles with the weighting parameter μ for the case $V_1 = \text{diag}(v_i^2)$ (the residual modes are not shown).

The robustness plots (Fig. 4) were drawn for all the optimized designs relative to various values of μ. It was found that, typically, low values of μ (low emphasis on performance) produced higher magnitudes in the high-frequency range of the $\bar{\sigma}(GK)$ curve. This demonstrates a tradeoff between spillover stabilization and performance degradation/stability robustness considerations. Nevertheless, for all the designs, the only violation of the robustness test involved the fourth mode, which was known to be stable.

Grid

As a multiple-input/multiple-output example, the two observer design procedures were also applied to a grid structure (Fig. 7) which is representative of a large space structure.[19] This structure is part of a research facility at Virginia Polytechnic Institute and State University. Its finite element model is described in Refs. 20 and 21. The natural frequencies of the first 20 modes are listed in Table 1. One notices a substantial frequency gap between modes 9 and 10. The control system assumed in this study (although different from the one used in the experimental facility) uses three collocated actuators and displacement sensors at locations 1, 4, and 11 and controls the first nine modes. Modes 10–20 act as residual modes and are used to evaluate the uncertainty. Both sets of modes are controllable and observable. The system input and output matrices can be found in Ref. 22, as well as the details of the LQR design (Q was selected to represent system energy, R designed using the MESS procedure). The actual noise environment was selected as W_1 and W_2 set to the unit matrices of the appropriate order.

Figure 8 shows the robustness plot for the design based on the actual noise statistics. The assumed damping is $\xi = 0.005$ for all modes. It can be seen that modes 10 and 11 violate the test, but modes 12 and above are robust. Consequently, only modes 10 and 11 have to be included as residuals in the KBF design procedure.

Another interesting observation from Fig. 8 is that the test is violated right within the bandwidth of the controller. This, of course, does not indicate a potential instability but is simply the consequence of the existence of transmission zeros of the open-loop system G very close to the imaginary axis. This results in the minimum singular value $\underline{\sigma}[G(j\omega)]$ becoming close to zero in Eq. (17). This behavior is typical of systems

Table 1 Grid structure example natural frequencies

Controlled, rad/s	ω_1	3.668
	ω_2	5.591
	ω_3	8.627
	ω_4	20.604
	ω_5	22.576
	ω_6	31.147
	ω_7	34.462
	ω_8	35.522
	ω_9	38.919
Residual, rad/s	ω_{10}	50.244
	ω_{11}	52.771
Robust, rad/s	ω_{12}	59.018
	ω_{13}	61.616
	ω_{14}	73.100
	ω_{15}	83.397
	ω_{16}	129.160
	ω_{17}	155.384
	ω_{18}	169.387
	ω_{19}	181.304
	ω_{20}	193.193

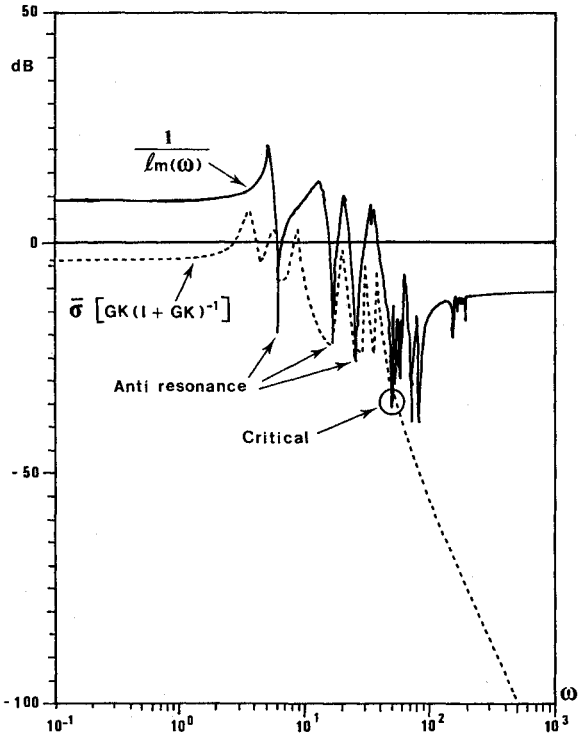

Fig. 8 Robustness plot for the grid structure (output uncertainty); the uncertainty curve corresponds to nodes 10-20; $\xi = 0.005$.

with collocated actuators and sensors. These "antiresonance" frequencies can be readily identified since they are identical to the natural frequencies of a modified structure in which the translational degree of freedom at locations 1, 4, and 11 is blocked.

Because of the large order of the system involved, the computer costs required a reduction in the number of design variables. For the diagonal case, V_1 was selected to be of the form (this is purely ad hoc)

$$V_1 = \text{diag}(a_v^2 a_v^2 a_v^2 b_v^2 b_v^2 b_v^2 c_v^2 c_v^2 c_v^2 d_v^2 d_v^2 d_v^2 e_v^2 e_v^2 e_v^2 f_v^2 f_v^2 f_v^2) \quad (26)$$

keeping the number of design variables to seven. This number proved to be effective for the previous example.

Table 2 Optimization results for $V_1 = \text{diag}(v_i^2)$, grid structure[a]

Weight	$\mu = 1000$	$\mu = 100$	$\mu = 10$
Observer poles	-3.955	-0.930	-0.819
	-22.296	-155.873	-259.587
	$-10.979 \pm j\,3.18$	-1.719	-1.501
	$-1.826 \pm j\,5.20$	-121.571	-209.333
	$-9.141 \pm j\,17.35$	$-3.530 \pm j\,5.15$	$-3.804 \pm j\,5.49$
	$-3.163 \pm j\,22.52$	$-12.629 \pm j\,17.26$	-17.031
	$-7.821 \pm j\,28.90$	$-3.194 \pm j\,21.74$	-38.878
	$-0.740 \pm j\,34.46$	$-5.576 \pm j\,28.99$	$-4.158 \pm j\,21.39$
	$-0.469 \pm j\,35.54$	$-0.859 \pm j\,34.48$	$-6.255 \pm j\,27.96$
	$-8.181 \pm j\,38.17$	$-0.488 \pm j\,35.54$	$-0.854 \pm j\,34.50$
		$-11.497 \pm j\,34.91$	$-0.467 \pm j\,35.53$
			$-12.002 \pm j\,32.32$
Residual poles (10th and 11th)	$-0.031 \pm j\,50.28$	$-0.072 \pm j\,50.28$	$-0.090 \pm j\,50.29$
	$-0.025 \pm j\,52.80$	$-0.062 \pm j\,52.81$	$-0.081 \pm j\,52.81$
J/J_{OPT}	1.0004	1.0093	1.0210

[a]System eigenvalues in 1/s.

Similarly, for the direct design of the observer gain matrix, K_c was constrained to the following form

$$K_c = \begin{bmatrix} a_k \begin{bmatrix} -0.978 \\ -0.084 \\ 1.109 \\ 0.551 \\ -0.352 \\ 0.921 \\ -0.437 \\ 0.437 \\ 0.476 \end{bmatrix} & c_k \begin{bmatrix} -0.618 \\ 1.119 \\ -0.494 \\ 0.867 \\ 0.780 \\ -0.533 \\ -0.801 \\ 0.756 \\ 0.457 \end{bmatrix} & e_k \begin{bmatrix} -0.773 \\ -0.497 \\ 0.034 \\ -0.572 \\ 1.115 \\ -0.246 \\ -0.714 \\ 0.246 \\ 0.717 \end{bmatrix} \\ b_k \begin{bmatrix} -0.049 \\ 0.518 \\ 0.573 \\ 0.180 \\ -0.052 \\ 0.732 \\ -0.455 \\ -0.815 \\ 0.460 \end{bmatrix} & d_k \begin{bmatrix} -0.183 \\ 0.410 \\ -0.237 \\ 0.748 \\ 0.104 \\ -0.491 \\ 0.497 \\ 0.658 \\ 0.861 \end{bmatrix} & f_k \begin{bmatrix} -0.168 \\ 0.242 \\ 0.374 \\ -0.161 \\ -0.107 \\ -0.172 \\ 0.451 \\ -0.280 \\ 0.313 \end{bmatrix} \end{bmatrix} \quad (27)$$

where, when $a_k = b_k = c_k = d_k = e_k = f_k = 1$, the statistical optimum gain matrix is obtained.

For the optimization, t was taken to equal $-0.100\ \text{s}^{-1}$, and $V_2 = \nu_1 [I + \nu_2 C_r C_r^T]$ via MESS[4,5] where $\nu_1 = 0.040$ and $\nu_2 = 1.0$. Therefore, $V_2 \neq W_2$ in this problem formulation. A tracing method was used for each of the designs, i.e., the optimum V_1 (or K_c) for one value of μ was used as the initial solution for the next value of μ.

The results for the observer design based on optimizing the matrices V_1 and K_c based on spillover and performance considerations are given in Fig. 9 and Table 2 as a function of the weighting parameter μ. Table 2 lists the observer poles, residual poles, and performance degradation. Note that the structural damping is not included in the real part of the residual pole since no damping is assumed in the controller design. As expected, as μ decreases in value, the performance index J

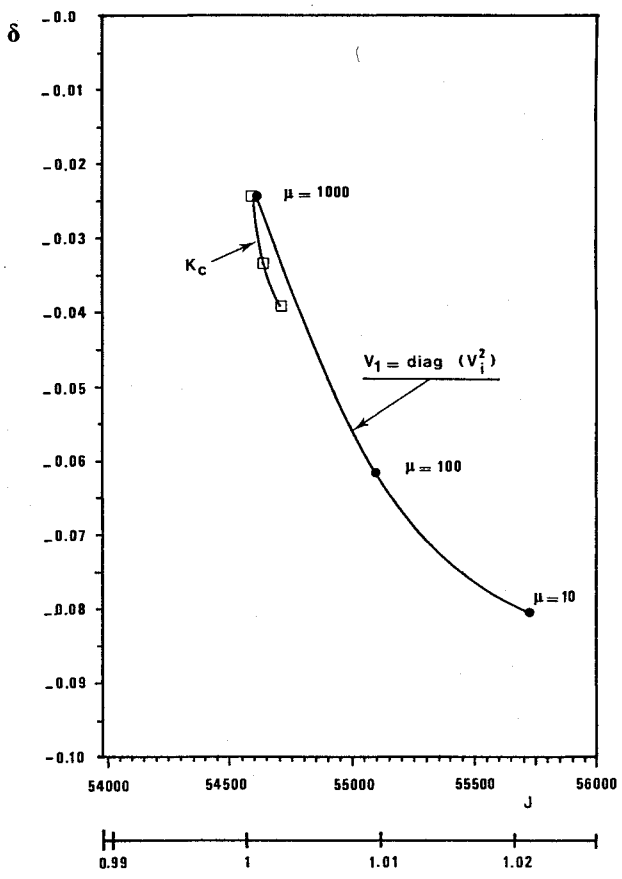

Fig. 9 Stability margin δ vs performance index J for various designs (grid structure).

increases in magnitude. At the same time, the system stability margin increases since the optimizer places more emphasis on a stable system at the cost of performance. It is shown that substantial gains in the stability of the residual modes can be obtained without a great loss of performance.

For initial conditions, V_1 was set as I, and K_c was set at the statistical optimum. For an extremely large μ, i.e., a heavy penalty is placed on performance in the optimization procedure, the fact that the K_c design produced the statistical optimum is not surprising. But for $V_1 = \text{diag}(v_i^2)$, even though $V_2 \neq W_2$ (it was defined by MESS), NEWSUMT-A was still able to produce an effective δ and J that were comparable to the statistical optimum. That is, $\delta = -0.0254$ s^{-1} and $J = 54606.0$ lb-s/in. for $V_1 = \text{diag}(v_i^2)$ vs $\delta = -0.02564$ s and $J = 54582$ lb-s/in. for the stochastic optimum.

Finally, stability robustness tests were also applied for $\xi = 0.005$. The robustness tests were performed using the knowledge of the first 20 modes of the grid in order to insure that the optimum controllers do not have any problems with the higher frequency modes, which were not taken into account in this analysis. All designs were found robust for modes 12 and above, with the classical observation that the closed-loop high-frequency behavior deteriorates (i.e., gets closer to the uncertainty curve) as the speed of the observer increases.

The computational cost for the three values of μ were 574 CPU minutes (IBM 3084) for the V_1 optimization and 145 min for the K_c optimization. This was mainly because the K_c optimization did not require the solution of the nonlinear Riccati equation.

Summary of the Proposed Design Procedure for Spillover Stabilization

Based on the results presented, the following design procedure is suggested.

1) Once the controlled modes have been selected, design an LQR to achieve a reasonable compromise between performance and control requirements, and a KBF with the best-available noise statistics.

2) Apply a robustness test where the uncertainty curve includes as many uncontrolled modes as possible and corresponds to a reasonable value of the structural damping.

3) Identify the uncontrolled modes that either fail the robustness test or have a small stability margin. These modes (residual) are candidates for spillover destabilization. If there are none, the design is completed.

4) Apply the foregoing optimization procedure to the design of an observer that stabilizes the modes identified in step 3 with respect to spillover.

5) Apply the robustness test to the new controller to check that it is satisfied by all the robust modes of the original controller, i.e., the robustness test is violated by at *most* the residual modes identified in step 3 and no more. These modes are guaranteed to be stable via the optimization process even though they fail the (conservative) robustness test. If this condition is met, the design is completed, if not, go back to step 4 with an augmented set of residual modes.

Conclusions

This paper considers the stabilization of the neglected dynamics of the higher modes of vibration. The influence of the structure of the plant noise intensity matrix of the Kalman-Bucy filter on the stability margin of the residual modes has been demonstrated. Stability robustness tests have been used to identify the potentially unstable uncontrolled modes. An optimization procedure that uses information on the residual modes to minimize spillover (i.e., maximize the stability margin) of known residual modes was presented. This procedure selects the optimum plant noise intensity matrix to maximize the stability margins of the residual modes without excessive performance degradation. An alternative procedure that directly optimizes the observer gain matrix was also discussed. The proposed methods were demonstrated for both single-input/single-output and multiple-input/multiple-output systems. It was found that only a small number of design variables was necessary in the optimization procedure to achieve large improvements in spillover stability.

In contrast to some other optimization schemes, the present method does not rely on obtaining a stable initial solution but can start with an unstable controller. There is no guarantee, however, that a stable solution can be achieved.

Acknowledgment

This work was supported in part by NASA Grant NAG-1-603.

References

[1]Balas, M. J., "Active Control of Flexible Systems," *Journal of Optimization Theory and Applications*, Vol. 25, No. 3, 1978, pp. 415-436.

[2] Canavin, J., "Control Technology of Large Space Structures," AIAA Paper 78-1691, Sept. 1978.

[3]Balas, M. J., "Enhanced Modal Control of Flexible Structures via Innovations Feedthrough," *International Journal of Control*, Vol. 32, No. 6, 1980, pp. 983-1003.

[4]Sesak, J. R., and Coradetti, T., "Decentralized Control of Large Space Structures via Forced Singular Perturbation," AIAA Paper 79-0195, Jan. 1979.

[5]Sesak, J. R., Likins, P., and Coradetti, T., "Flexible Spacecraft Control by Model Error Sensitivity Suppression," *Second Virginia Polytechnic Institute and State University/AIAA Symposium on Dynamics and Control of Large Flexible Spacecraft*, Virginia Polytechnic Inst. and State Univ., Blacksburg, VA, July 1979, pp. 349-368.

[6]Gupta, N. K., "Frequency-Shaped Cost Functional Extension of Linear-Quadratic-Gaussian Design Methods," *Journal of Guidance and Control*, Vol. 3, No. 6, 1980, pp. 529-535.

[7]Preumont, A., "Spillover Alleviation in Active Control of Flexible Structures," *Journal of Guidance and Control,* Vol. 11, No. 2, 1988, pp. 124–130.

[8]Kwakernaak, H., and Sivan, R., *Linear Optimal Control Systems,* Wiley-Interscience, New York, 1972.

[9]Mukhopadhyay, V., Newsom, J. R., and Abel, I., "Reduced Order Optimal Feedback Control Law Synthesis for Flutter Suppression," *Journal of Guidance, Control and Dynamics,* Vol. 5, No. 4, 1982, pp. 389–395.

[10]Newsom, J. R., and Mukhopadhyay, V., "Application of Constrained Optimization to Active Control of Aeroelastic Response," NASA TM 83150, June 1981.

[11]Ridgely, D. B., and Banda, S. S., "Introduction to Robust Multivariable Control," Air Force Wright Aeronautics Labs., Wright-Patterson AFB, OH, AFWAL-TR-85-3102, Feb. 1986.

[12]Doyle, J. C., and Stein, G., "Multivariable Feedback Design: Concepts for a Classical/Modern Synthesis," *IEEE Transactions on Automatic Control,* Vol. AC-26, No. 1, 1981, pp. 4–15.

[13]Kissel, G. J., and Hegg, D. R., "Stability Enhancement for Control of Flexible Space Structures," *IEEE Control Systems Magazine,* Vol. 6, June 1986, pp. 19–26.

[14]Joshi, S. M., Rowell, L. F., and Armstrong, E. S., "Robust Controller Synthesis for Large Flexible Space Structures," *Recent Advances in Control of Nonlinear and Distributed Parameter Systems, Robust Control, and Aerospace Control Applications,* edited by J. Bentsman and S. M. Joshi, American Society of Mechanical Engineers, New York, DSC Vol. 10, 1988, pp. 147–156.

[15]Balas, M. J., Quan, R., Davidson, R., and Das, B., "Low-Order Control of Large Aerospace Structures Using Residual Mode Filters," *Recent Advances in Control of Nonlinear and Distributed Parameter Systems, Robust Control, and Aerospace Control Applications,* edited by J. Bentsman and S. M. Joshi, American Society of Mechanical Engineers, New York, DSC Vol. 10, 1988.

[16]Czajkowski, E., and Preumont, A., "Spillover Stabilization and Decentralized Modal Control of Large Space Structures," *Proceedings of the AIAA Dynamics Specialist Conference,* AIAA, New York, April 1987, pp. 599–609.

[17]Grandhi, R. V., Thareja, R., and Haftka, R. T., "NEWSUMT-A: A General Purpose Program for Constrained Optimization Using Constraint Approximations," *Journal of Mechanics, Transmission and Automation in Design,* Vol. 107, March 1985, pp. 94–99.

[18]Bingulac, S. P., West, P. J., and Perkins, W. R., "Recent Advances in the L-A-S Software Used in CAD of Control Systems," *Third IFAC Symposium on CAD in Control,* Copenhagen, July 1985, pp. 124–129.

[19]Hallauer, W. L., Jr., Skidmore, G. R., and Gehling, R. N., "Modal-Space Active Damping of a Plane Grid: Experiment and Theory," *Journal of Guidance, Control, and Dynamics,* Vol. 8, No. 3, 1985, pp. 366–373.

[20]Masse, M. A., "A Plane Grillage Model for Structural Dynamics Experiments: Design, Theoretical Analysis, and Experimental Testing," M.S. Thesis, Virginia Polytechnic Inst. and State Univ., Blacksburg, VA, Feb. 1983.

[21]Gehling, R. N., "Experimental and Theoretical Analysis of a Plane Grillage Structure with High Modal Density," M.S. Thesis, Virginia Polytechnic Inst. and State Univ., Blacksburg, VA, March 1984.

[22]Czajkowski, E. A., "Spillover Stabilization in the Control of Large Flexible Space Structures," Ph.D. Dissertation, Virginia Polytechnic Inst. and State Univ., Blacksburg, VA, May 1988.